We are IntechOpen,
the world's leading publisher of
Open Access books
Built by scientists, for scientists

6,900
Open access books available

186,000
International authors and editors

200M
Downloads

154
Countries delivered to

Our authors are among the

TOP 1%
most cited scientists

12.2%
Contributors from top 500 universities

WEB OF SCIENCE™

Selection of our books indexed in the Book Citation Index
in Web of Science™ Core Collection (BKCI)

Interested in publishing with us?
Contact book.department@intechopen.com

Numbers displayed above are based on latest data collected.
For more information visit www.intechopen.com

Biotribology of Mechanically and Laser Marked Biomaterial

Marcelo de Matos Macedo, Vikas Verma,

Jorge Humberto Luna-Domínguez and Ronaldo Câmara Cozza

Abstract

The purpose of present work is to study the biotribological behavior of a mechanically and laser marked biomaterial. Sliding wear tests were conducted on ASTM F139 austenitic stainless-steel specimen, with polypropylene and AISI 316 L austenitic stainless-steel balls, as counterbodies. During wear experiments, a liquid chemical composition was continuously fed between the specimen and the ball. The coefficient of friction acting on the tribological system "specimen – liquid chemical composition – ball" and the wear volume of the wear craters were calculated, and results were analyzed. The results have shown that the biotribological behavior of ASTM F139 austenitic stainless steel was influenced by mechanical or laser marking process, and its wear resistance was dependent on the kind of counterbody.

Keywords: biomaterial, austenitic stainless steel, laser treatment, wear resistance, wear volume, coefficient of friction

1. Introduction

The "ball-cratering wear test" has gained large acceptance at universities and research centers as it is widely used in studies focusing on the wear behavior of different materials [1–20]. **Figure 1** presents a schematic diagram of the principle of wear test, where a rotating ball is forced against the tested specimen and liquid solution supplied between the specimen and the ball during the experiments.

The aim of the "ball-cratering wear test" is to generate "wear craters" on the surface of the specimen. **Figure 2** presents an image of such crater, together with an indication of the crater diameter (d) (**Figure 2a**) and the wear volume (V) (**Figure 2b** [21]). The wear volume is determined as a function of "d," using Eq. (1) [22], where R is the radius of the ball.

$$V \cong \frac{\pi d^4}{64R} \text{ for } d << R \tag{1}$$

In other line of research, the concept of "biotribology" has gained important spotlight in the area, including research works addressing the biotribological behavior of materials [23–29] used in the manufacturing of human body elements. Consequently, different laboratory techniques have been employed to reproduce conditions where there are friction and consequent wear of parts of the human mechanical structure with relative movement.

1

However, wear tests conducted under the "ball-cratering" technique present advantages in relation to other types of tribological procedures, as it favors the desired analysis of the tribological behavior. Therefore, considering the need of tribological characterization of biomaterials and the capacity that the "ball-cratering wear test" method presents to this goal, the purpose of this work is to study the biotribological behavior of mechanically and laser-marked ASTM F139 austenitic stainless-steel biomaterial.
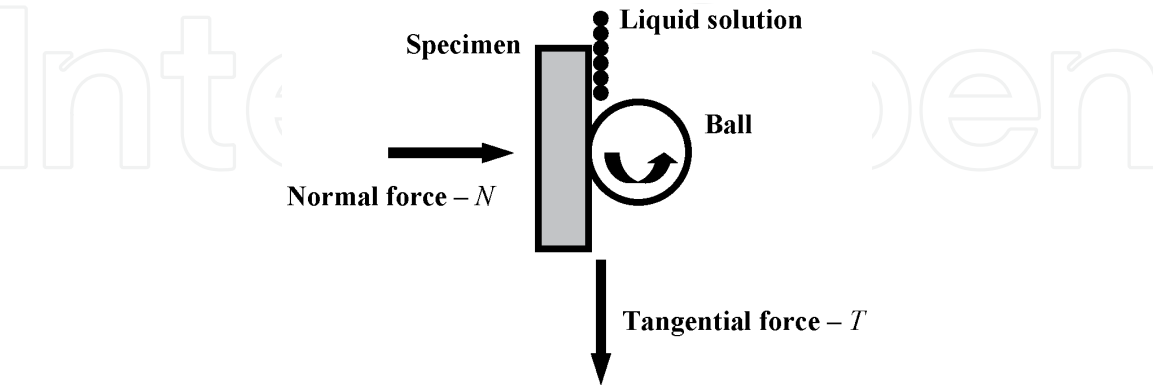
Figure 1.
"Ball-cratering wear test": representative figure of its operating principle.
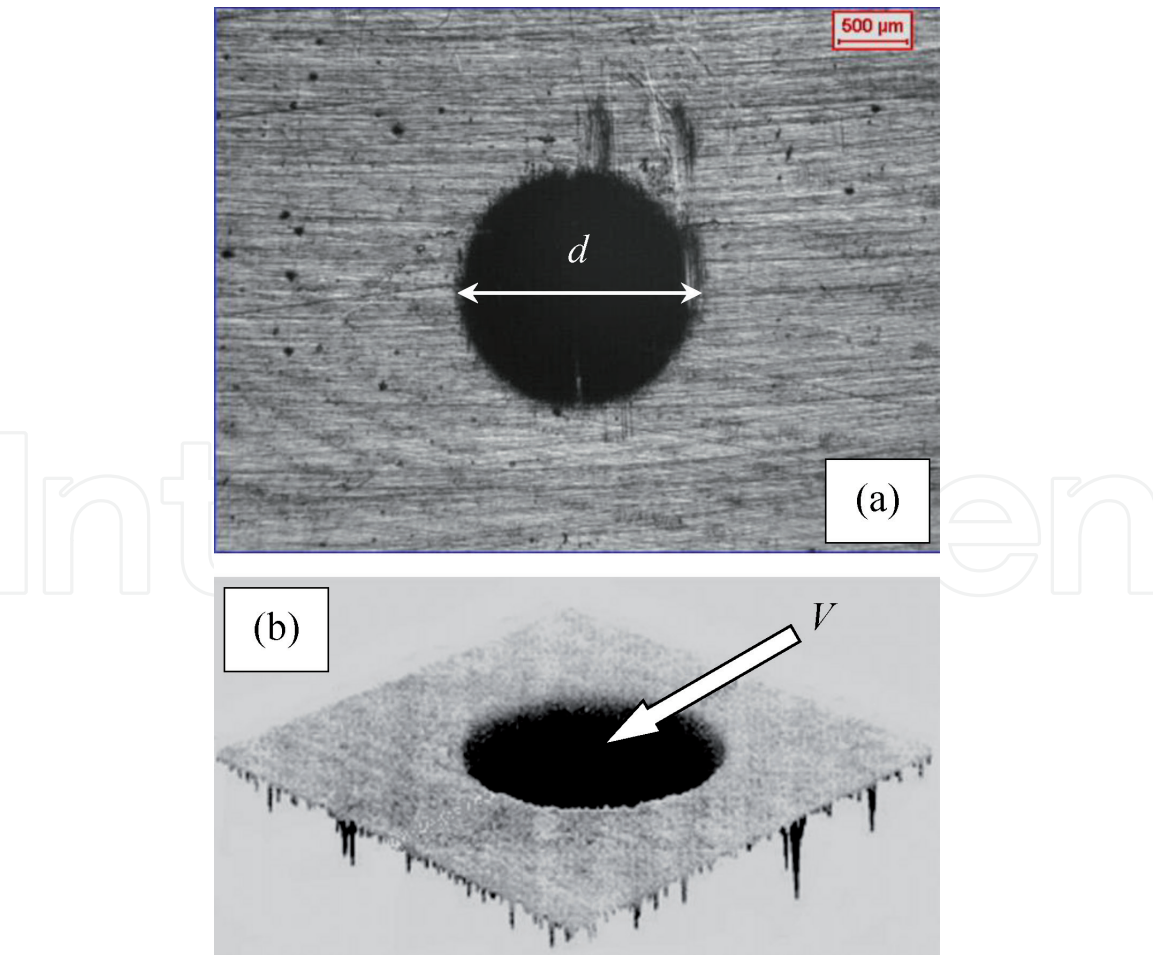
Figure 2.
Images of wear craters: (a) diameter – d and (b) wear volume – V [21].

2. Experimental details

2.1 Ball-cratering wear test equipment

Equipment with free-ball mechanical configuration (**Figure 3a**) was used for the sliding wear tests. Two load cells were used in the tribometer: one load cell to control the "normal force – N" applied on the specimen (**Figure 3b**) and the other load cell to measure the "tangential force – T" developed during the experiments (**Figure 3c**).

"Normal" and "tangential" force load cells have a maximum capacity of 50 N and an accuracy of 0.001 N. The values of N and T were registered by a data acquisition system, in real time, during the sliding wear tests.

2.2 Materials

The tested specimen was an ASTM F139 austenitic stainless-steel biomaterial, marked mechanically and with a nanosecond Q-switched Nd: YAG laser. Its chemical composition is presented in **Table 1**.

Balls of polypropylene and AISI 316 L austenitic stainless steel, with diameter of $D = 25.4$ mm ($D = 1''$ – standard size), were adopted as counterbodies.

To simulate the fluid present in the human body, a chemical liquid solution of PBS – Phosphate Buffered Solution – was inserted between the specimen and the ball. It was composed by the materials mentioned in **Table 2**.

Table 3 shows the hardness (H) of the materials used in this work (specimen and test balls).

2.3 Ball-cratering wear tests and data acquisition

Table 4 presents the test conditions defined for the sliding wear experiments conducted in this research.

Following values of normal force (N) for the sliding wear experiments: $N_{PP} = 0.05$ N and $N_{316L} = 0.40$ N were defined as a function of density (ρ) of the ball material – polypropylene $\Rightarrow \rho_{PP} = 0.91$ g/cm^3 and AISI 316 L austenitic stainless steel $\Rightarrow \rho_{316L} = 8$ g/cm^3. The rotational speed (n) of ball was 75 rpm. For $n = 75$ rpm and $D = 25.4$ mm, the tangential sliding velocity (v) of the ball is 0.1 m/s. Wear tests were conducted under a test time (t) of 10 min. With 0.1 m/s tangential sliding velocity and 10 min (600 s) test time, a sliding distance (S) of 60 m was calculated between the ball and the specimen.

All experiments were conducted without interruption, and the chemical liquid solution of PBS – Phosphate Buffered Solution – was fed between the specimen and the ball during the tests, under a frequency of 1 drop/10 s. Both the normal force (N) and the tangential force (T) were monitored and registered constantly. Finalizing the sliding wear tests, the diameters (d) of the wear craters were measured by optical microscopy, and their surfaces were analyzed by scanning electron microscopy.
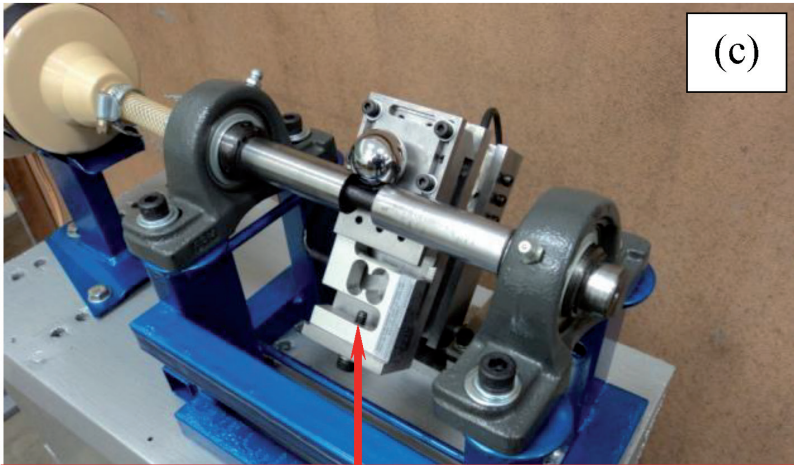
Finally, the wear volume (V) was calculated by Eq. (1), and the coefficient of friction (μ) was determined using Eq. (2):

$$\mu = \frac{T}{N} \qquad (2)$$
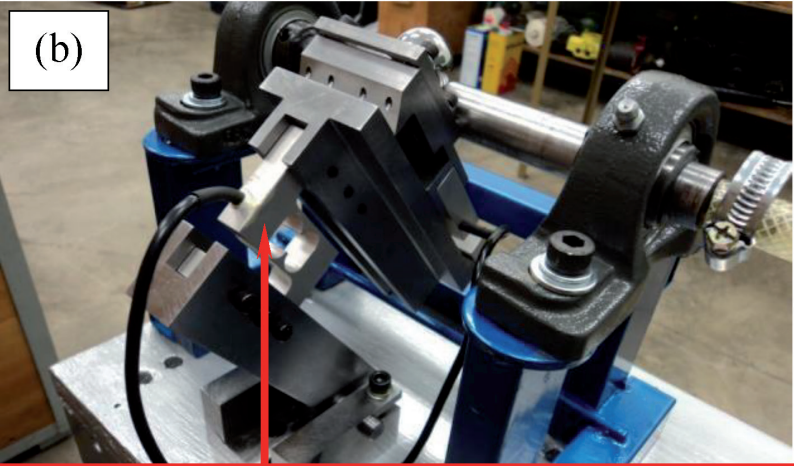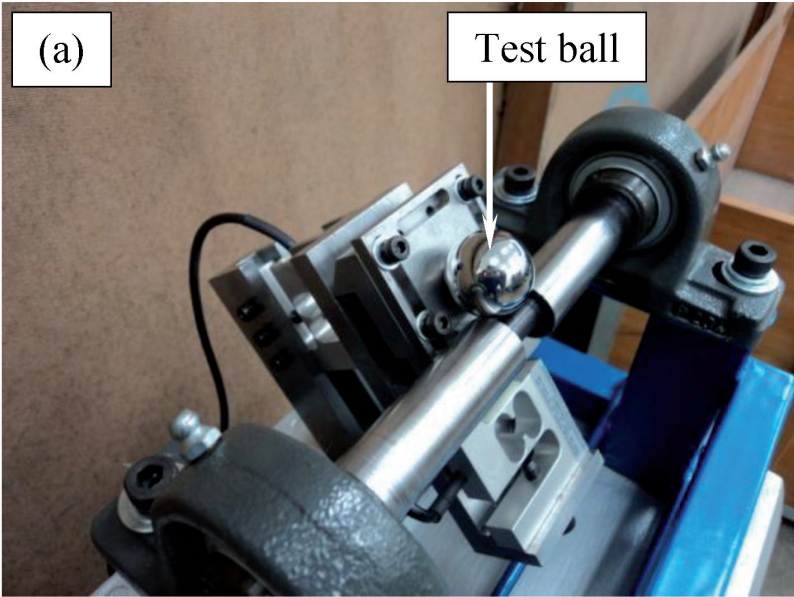
Figure 3.
(a) "Ball-cratering" wear test equipment with "free-ball" mechanical configuration used for the sliding wear tests: (b) load cell mounted to control the normal force and (c) load cell positioned to measure the tangential force during the experiments.

Chemical element	% (in weight)
C	0.023
Si	0.78
Mn	2.09
P	0.026
S	0.0003
Cr	18.32
Mo	2.59
Ni	14.33
Fe	Balance

Table 1.
Chemical composition of ASTM F139 austenitic stainless-steel biomaterial – in percentage weight.

Chemical element	(g/l)
NaCl	8
KCl	0.2
Na_2HPO_4	1.15
KH_2PO_4	0.2

Table 2.
Chemical composition of the PBS – phosphate buffered solution – in g/l.

	Material	Hardness – H
Specimen	ASTM F139 austenitic stainless steel	180 HV
Test ball	Polypropylene	55 – Shore D
	AISI 316 L austenitic stainless steel	318 HV

Table 3.
Hardness of the materials used in this work.

Normal force – N_{PP}	Ball of polypropylene	0.05 N
Normal force – N_{316L}	Ball of AISI 316 L austenitic stainless steel	0.40 N
Test ball rotational speed – n		75 rpm
Tangential sliding velocity – v		0.1 m/s
Test time – t		10 min
Sliding distance – S		60 m

Table 4.
Test parameters for the ball-cratering wear tests under conditions of sliding wear.
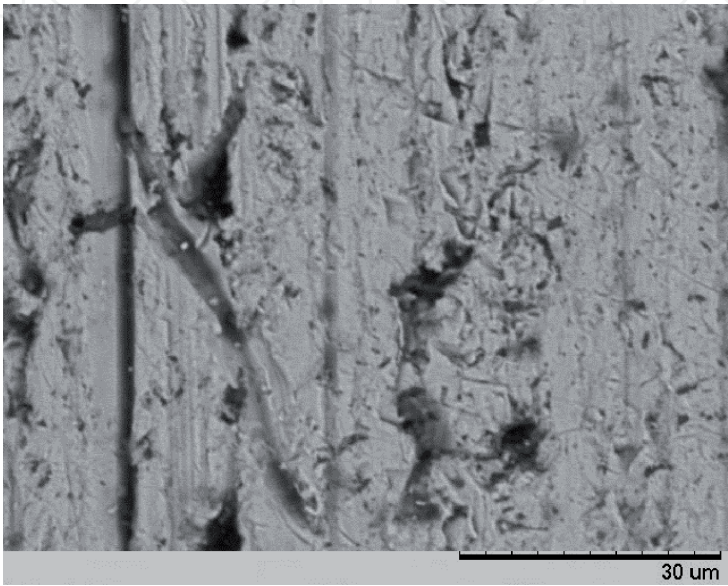
3. Results and discussion

3.1 Scanning electron microscopy

Figure 4 shows a scanning electron micrograph of the surface of a wear crater generated during the sliding wear tests.

Occurrence of grooves, due to sliding movement between the ball and the specimen, was observed in the scanning electron micrograph. The result presented in **Figure 4** is in qualitative agreement with the literature [30], where it is reported that the action of grooves on the surface of a material is characterized as a common tribological behavior of two metallic materials under relative movement.

3.2 Wear volume behavior

Figure 5 presents the behavior of the specimen in terms of wear volume (V) for the following conditions: mechanically and laser-marked specimen and different types of balls (counterbodies).

Figure 4.
Scanning electron micrograph of the surface of a wear crater generated during the sliding wear tests.
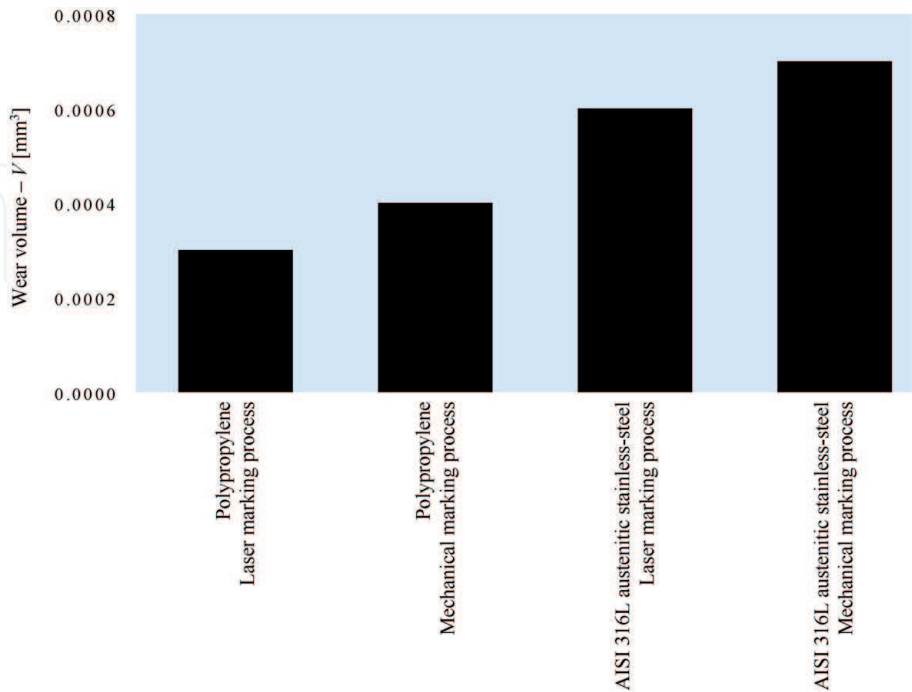
Figure 5.
Wear volume (V) behavior as a function of the type of marking process ("mechanical" or "laser") and type of counterbody (ball of polypropylene or ball of AISI 316 L austenitic stainless steel). Maximum standard deviation reported: ±7 × 10^{-4} mm^3.
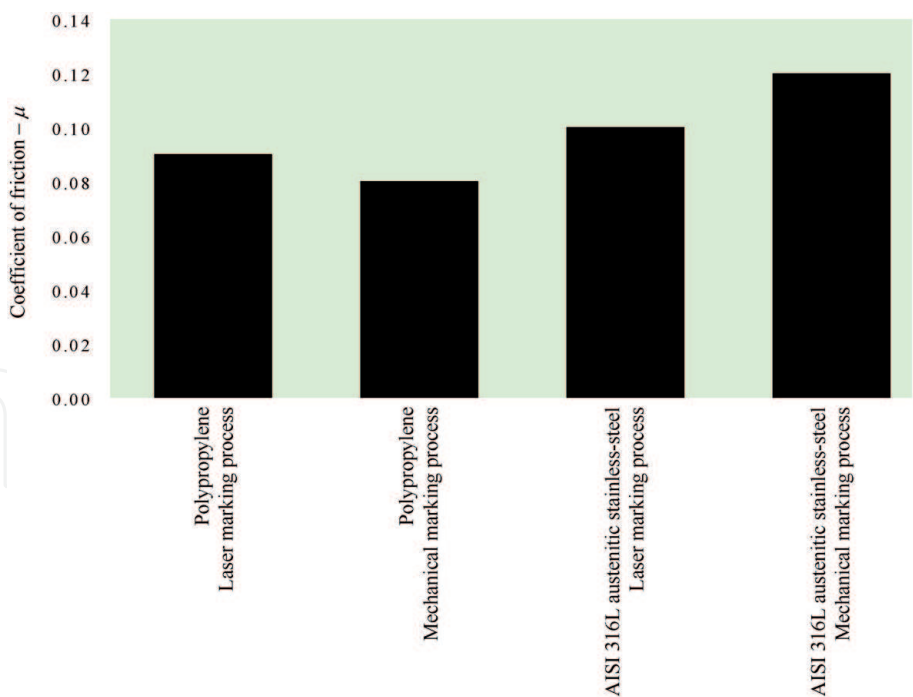
Figure 6.
Coefficient of friction behavior (μ) as a function of the type of marking process ("mechanical" or "laser") and type of counterbody (ball of polypropylene or ball of AISI 316 L austenitic stainless steel). Maximum standard deviation reported: ±0.03.

In addition, **Figure 5** shows a decrease in wear volume under laser marking process for both types of counterbodies. Decrease in wear volume is related to increase in local hardness of the specimen. Increase of hardness can be attributed to the action of laser on specimen surface. In relation to specimen marked mechanically, the possible increase of local hardness could have occurred due to local surface hardening.

However, the increase of local hardness caused by laser marking is higher than the local hardness caused by mechanical marking, justifying the results presented in **Figure 5**.

3.3 Coefficient of friction behavior

Figure 6 shows the behavior of the coefficient of friction (μ) for the conditions, which the specimen is marked mechanically and marked with laser, and for the different types of balls – counterbodies.

In the present tribological conditions, coefficient of friction was found lower for the wear tests conducted against polypropylene ball than AISI 316 L austenitic stainless-steel ball counterbodies.

4. Conclusions

The following conclusions can be drawn from the results obtained in this research, regarding to tribological behavior of ASTM F139 austenitic stainless steel:

- tribological behavior was influenced by the type of the marking process – "mechanical" or "laser" – applied for the investigated biomaterial;

- wear volume was found to be dependent on the normal force acting on the specimen, that is, they were dependent on the type of counterbody – ball of polypropylene or ball of AISI 316 L austenitic stainless steel; and

- coefficient of friction was found dependent on the type of ball; the lower values of μ were observed under the use of polypropylene ball.

Nomenclature

d	diameter of the wear crater (mm)
D	diameter of the test ball (mm)
H	hardness (HV)
n	test ball rotational speed (rpm)
N	normal force (applied on the specimen) (N)
R	radius of the test ball (mm)
S	sliding distance (m)
t	test time (min)
T	tangential force (developed during the wear tests) (N)
v	tangential sliding velocity of the test ball (m/s)
V	wear volume of the wear crater (mm^3)

Greek letters

μ	coefficient of friction
ρ	density (g/cm^3)

Author details

Marcelo de Matos Macedo[1], Vikas Verma[2], Jorge Humberto Luna-Domínguez[3] and Ronaldo Câmara Cozza[1,4*]

1 Department of Mechanical Manufacturing, Technology Faculty – FATEC-Mauá, CEETEPS – State Center of Technological Education "Paula Souza", Mauá, SP, Brazil

2 Thermochemistry of Materials SRC, National University of Science and Technology (NUST) MISiS, Moscow, Russia

3 Facultad de Odontología, Universidad Autónoma de Tamaulipas, Tamaulipas, Mexico

4 Department of Mechanical Engineering, University Center FEI – Educational Foundation of Ignatius "Padre Sabóia de Medeiros", SP, Brazil

*Address all correspondence to: rcamara@fei.edu.br

IntechOpen

References

[1] Cozza RC. A study on friction coefficient and wear coefficient of coated systems submitted to micro-scale abrasion tests. Surface & Coatings Technology. 2013;**215**:224-233. DOI: 10.1016/j.surfcoat.2012.06.088

[2] Cozza RC, Rodrigues LC, Schön CG. Analysis of the micro-abrasive wear behavior of an iron aluminide alloy under ambient and high-temperature conditions. Wear. 2015;**330-331**:250-260. DOI: 10.1016/j.wear.2015.02.021

[3] Cozza RC, JTSL W, Schön CG. Influence of abrasive wear modes on the coefficient of friction of thin films. Tecnologia em Metalurgia, Materiais e Mineração. 2018;**15**(4):504-509. DOI: 10.4322/2176-1523.20181468

[4] Umemura MT, Jiménez LBV, Pinedo CE, Cozza RC, Tschiptschin AP. Assessment of tribological properties of plasma nitrided 410S ferritic-martensitic stainless steels. Wear. 2019;**426-427**:49-58. DOI: 10.1016/j.wear.2018.12.092

[5] Cozza RC. Thin films: Study of the influence of the micro-abrasive wear modes on the volume of wear and coefficient of friction. In: Friction, Lubrication and Wear. 1st ed. London–UK: IntechOpen; 2019. DOI: 10.5772/intechopen.86459

[6] Cozza RC. Effect of pressure on abrasive wear mode transitions in micro-abrasive wear tests of WC-Co P20. Tribology International. 2013;**57**:266-271. DOI: 10.1016/j.triboint.2012.06.028

[7] Cozza RC. Effect of sliding distance on abrasive wear modes transition. Journal of Materials Research and Technology. 2015;**4**(2):144-150. DOI: 10.1016/j.jmrt.2014.10.007

[8] Wilcken JTSL, Silva FA, Cozza RC, Schön CG. Influence of abrasive wear modes on the coefficient of friction of thin films. In: Proceedings of the "ICAP 2014 – 2nd International Conference on Abrasive Processes". Cambridge – UK: The University of Cambridge; September 8-10, 2014

[9] Cozza RC. Study of the steady-state of wear in micro-abrasive wear tests by rotative ball conducted on specimen of WC-Co P20 and M2 tool-steel. Revista Matéria. 2018;**23**(1):e-11986. DOI: 10.1590/s1517-707620170001.0322

[10] da Silva WM, Binder R, de Mello JDB. Abrasive wear of steam-treated sintered iron. Wear. 2005;**258**:166-177. DOI: 10.1016/j.wear.2004.09.042

[11] Trezona RI, Allsopp DN, Hutchings IM. Transitions between two-body and three-body abrasive wear: Influence of test conditions in the microscale abrasive wear test. Wear. 1999;**225-229**:205-214. DOI: 10.1016/S0043-1648(98)00358-5

[12] Adachi K, Hutchings IM. Wear-mode mapping for the micro-scale abrasion test. Wear. 2003;**255**:23-29. DOI: 10.1016/S0043-1648(03)00073-5

[13] Adachi K, Hutchings IM. Sensitivity of wear rates in the micro-scale abrasion test to test conditions and material hardness. Wear. 2005;**258**:318-321. DOI: 10.1016/j.wear.2004.02.016

[14] Cozza RC, de Mello JDB, Tanaka DK, Souza RM. Relationship between test severity and wear mode transition in micro-abrasive wear tests. Wear. 2007;**263**:111-116. DOI: 10.1016/j.wear.2007.01.099

[15] Cozza RC, Tanaka DK, Souza RM. Micro-abrasive wear of DC and pulsed DC titanium nitride thin films with different levels of film residual stresses. Surface and Coatings Technology.

2006;**201**:4242-4246. DOI: 10.1016/j.surfcoat.2006.08.044

[16] Bose K, Wood RJK. Optimun tests conditions for attaining uniform rolling abrasion in ball cratering tests on hard coatings. Wear. 2005;**258**:322-332. DOI: 10.1016/j.wear.2004.09.018

[17] Mergler YJ, Huis in 't Veld AJ. Micro-abrasive wear of semi-crystalline polymers. Tribology and Interface Engineering Series. 2003;**41**:165-173. DOI: 10.1016/S0167-8922(03)80129-3

[18] Batista JCA, Matthews A, Godoy C. Micro-abrasive wear of PVD duplex and single-layered coatings. Surface and Coatings Technology. 2001;**142-144**:1137-1143. DOI: 10.1016/S0257-8972(01)01189-6

[19] Batista JCA, Godoy C, Matthews A. Micro-scale abrasive wear testing of duplex and non-duplex (single-layered) PVD (Ti,Al)N, TiN and Cr-N coatings. Tribology International. 2002;**35**:363-372. DOI: 10.1016/S0301-679X(02)00017-8

[20] Batista JCA, Joseph MC, Godoy C, Matthews A. Micro-abrasion wear testing of PVD TiN coatings on untreated and plasma nitrided AISI H13 steel. Wear. 2002;**249**:971-979. DOI: 10.1016/S0043-1648(01)00833-X

[21] da Silva WM. Effect of pressing pressure and iron powder size on the micro-abrasion of steam-oxidized sintered iron [M.Sc. Dissertation]. Uberlândia–MG, Brazil: Federal University of Uberlândia; 2003. p. 98

[22] Rutherford KL, Hutchings IM. Theory and application of a micro-scale abrasive wear test. Journal of Testing and Evaluation. 1997;**25**(2):250-260. DOI: 10.1520/JTE11487J

[23] Niinomi M, Nakai M, Hieda J. Development of new metallic alloys for biomedical applications. Acta Biomaterialia. 2012;**8**:3888-3903. DOI: 10.1016/j.actbio.2012.06.037

[24] Talha M, Behera CK, Sinha OP. A review on nickel-free nitrogen containing austenitic stainless steels for biomedical applications. Materials Science and Engineering C. 2013;**33**:3563-3575. DOI: 10.1016/j.msec.2013.06.002

[25] Gurappa I. Development of appropriate thickness ceramic coatings on 316 L stainless steel for biomedical applications. Surface and Coatings Technology. 2002;**161**:70-78. DOI: 10.1016/S0257-8972(02)00380-8

[26] Shih CC, Shih CM, Su YY, LHJ S, Chang MS, Lin SJ. Effect of surface oxide properties on corrosion resistance of 316L stainless steel for biomedical applications. Corrosion Science. 2004;**46**:427-441. DOI: 10.1016/S0010-938X(03)00148-3

[27] Hosseinalipour SM, Ershad-Langroudi A, Hayati AN, Nabizade-Haghighi AM. Characterization of sol–gel coated 316L stainless steel for biomedical applications. Progress in Organic Coatings. 2010;**67**:371-374. DOI: 10.1016/j.porgcoat.2010.01.002

[28] Dewidar MM, Khalil KA, Lim JK. Processing and mechanical properties of porous 3 16L stainless steel for biomedical applications. Transactions of Nonferrous Metals Society of China. 2007;**17**(3):468-473. DOI: 10.1016/S1003-6326(07)60117-4

[29] Niinomi M. Recent metallic materials for biomedical applications. Metallurgical and Materials Transactions A. 2002;**33A**:477-486. DOI: 10.1007/s11661-002-0109-2

[30] Cozza RC. Third abrasive wear mode: Is it possible? Journal of Materials Research and Technology. 2014;**3**(2):191-193. DOI: 10.1016/j.jmrt.2014.03.010